Scale of Acidities in the Gas Phase from Methanol to Phenol

John E. Bartmess, Judith A. Scott, and Robert T. McIver, Jr.*

Contribution from the Department of Chemistry, University of California, Irvine, California 92717. *Received February 13, 1979*

Abstract: The relative gas-phase acidities of 81 oxygen, nitrogen, carbon, sulfur, and phosphorus acids have been measured at 320 K with a pulsed ion cyclotron resonance spectrometer. Equilibrium constants for reactions of the general type $A^- + BH = B^- + AH$ are used to determine the relative acidities of the two acids AH and BH in the absence of solvation. The experimental data are also used to calculate gaseous heats of formation for a wide variety of anions, $\Delta H°_f(A^-)$, electron affinities of radicals, EA (A·), and bond dissociation energies, DH°(A–H). Criteria for the establishment of equilibrium in pulsed ICR experiments are discussed.

There exists in the literature an extensive body of thermochemical data for organic cations in the gas phase.[1] These data have been derived primarily from ionization potentials and appearance potentials measured by electron impact and photoionization mass spectrometry. More recently, thermochemical data for positive ions have also become available from gaseous ion-molecule reactions studied by high pressure mass spectrometry,[2] flowing afterglow,[3] and ion cyclotron resonance (ICR) spectrometry.[4] In particular, equilibrium proton transfer reactions have provided extensive data for the basicity of molecules in the gas phase, and valuable insight into the nature of solvation effects has been gained by comparing solution phase and gas phase basicities.[5]

In contrast to this, very little is known about the thermochemistry of anions in the gas phase. Negative ions can be detected by electron impact and photoionization mass spectrometry, but the cross section for their production is typically about a thousand times less than for production of positive ions.[6] Furthermore, negative ions produced by electron impact often have excess translational energy which hinders their collection in sector-type instruments. For these reasons, measurement of thresholds for production of negative ions has not been nearly as fruitful as for positive ions. Fortunately, however, a number of other techniques have proved to be more easily adapted for thermochemical studies of gaseous negative ions. For example, thresholds for photodetachment of electrons from negative ions

$$A^- + h\nu \rightarrow A\cdot + e^- \tag{1}$$

can be determined by varying either the wavelength of the incident light[7] or by measuring the translational energy of the detached electron.[8] These experiments provide data for the electron affinities of radicals, and heats of formation of negative ions and radicals. A wide variety of negative ion-molecule reactions in the gas phase have also been used to derive thermochemical data. For example, relative electron affinities can be determined by measuring the translational energy threshold for endothermic reactions such as[9]

$$\begin{gathered} I^- + M \rightarrow M^{-}\cdot + I\cdot \\ Cs + M \rightarrow M^{-}\cdot + Cs^+\cdot \end{gathered} \tag{2}$$

or by measuring equilibrium constants for gas-phase electron transfer reactions such as[10]

$$M_1^{-}\cdot + M_2 = M_2^{-}\cdot + M_1\cdot \tag{3}$$

Relative acidities of molecules in the gas phase have been determined in high pressure mass spectrometers,[11] flowing afterglow reactors,[12] and pulsed ICR spectrometers[13] by measuring equilibrium constants K for proton transfer reactions such as

$$A^- + BH = B^- + AH \tag{4}$$

The standard Gibb's free energy change for this reaction, $\delta\Delta G°_{acid} = -RT \ln K$, is a measure of the relative acidity of AH and BH in the gas phase. A series of acids can be studied to establish a scale of relative acidities in the same manner as pK_a values are determined in solution. In addition, an absolute scale corresponding to the process

$$AH = A^- + H^+ \tag{5}$$

can be established by incorporating into the relative scale certain standards such as $H_2 = H^- + H^+$ and $HF = F^- + H^+$ for which $\Delta H°_{acid}$ and $\Delta G°_{acid}$ can be calculated from available data. Measurement of gas phase acidities in this way provides through reaction 5 a potentially powerful and general route to heats of formation of anions.

In this paper we report the relative gas-phase acidities of 81 oxygen, nitrogen, carbon, sulfur, and phosphorus acids. The compounds chosen for this study encompass a wide range of interesting structures and serve to complement the other quantitative gas phase acidity studies which have been reported.[11-13] An absolute scale of acidities from methanol to phenol is constructed with several standards included, and the data are used to calculate heats of formation of anions, electron affinities of radicals, and bond dissociation energies DH°(A–H). In addition, the pulsed ICR technique used in the measurements is described in detail and subjected to several classical tests for the attainment of equilibrium. An analysis of structural effects on gas-phase acidities is presented in the paper which follows this one.

Experimental Section

The gas-phase acidity measurements reported in this paper were performed with a pulsed ion cyclotron resonance (ICR) mass spectrometer which was designed and constructed in our laboratory at the University of California, Irvine. The pulsed ICR technique utilizes the cyclotron resonance principle for mass analysis of gaseous ions stored in a one-region trapped ICR cell.[14] At a typical operating pressure of 5×10^{-6} Torr, ions are stored efficiently for about 1 s by a homogeneous magnetic field of 1.4 T and a weak (0.5 V/cm) electric field. All of the operations of ion formation, trapping, double resonance irradiation, and mass analysis are performed in the one-region ICR cell using a pulsed mode of operation.[15] Most of the experimental techniques are the same as were used in this laboratory for construction of the gas-phase basicity scale from H_2O to NH_3.[4a] Only the additional techniques needed for studying negative ions will be described here.

The one-region ICR cell will trap either positive ions or negative ions, depending upon the polarity of the voltages applied to the plates of the cell. For negative ion studies, the two side plates (those perpendicular to the magnetic field) are set typically at −1.0 V, and the other four plates are set at +0.5 V. This establishes an 0.7-V electrostatic potential well at the center of the cell in the direction parallel to the magnetic field. All negatively charged particles are trapped, regardless of *m/e*.

Since most of the compounds studied here do not form negative ions efficiently upon direct electron impact, a third compound such as

0002-7863/79/1501-6046$01.00/0

CH_3ONO, H_2O, or NH_3 was added to serve as a source of negative ions. Scheme I illustrates in general the reactions which occur. An experiment is initiated by a short pulse (about 10 ms) of electrons through the center of the ICR cell. Compound XY captures the electrons and undergoes dissociative electron capture, reaction 6, to produce the anionic base X^-. Methyl nitrite was used as the source of CH_3O^- for most of the experiments reported here. It has a very large cross section for capture of low energy (<0.2 eV) electrons,[16] and its partial pressure could be kept at less than 1×10^{-7} Torr. The next step, reactions 7, is rapid, irreversible deprotonation of the acids AH and BH, which have been added to partial pressures on the order of 10^{-6} Torr. Reaction 7 is usually complete in about 10 to 50 ms.

Scheme I

$$e^- + XY \rightarrow X^- + Y\cdot \quad (6)$$

$$X^- + AH \rightarrow A^- + HX \quad (7)$$

$$X^- + BH \rightarrow B^- + HX$$

$$A^- + BH \underset{k_{-1}}{\overset{k_1}{\rightleftharpoons}} B^- + AH \quad (8)$$

$$A^- + M \xrightarrow{k_{loss}} \text{ion loss} \quad (9)$$

$$B^- + M \xrightarrow{k'_{loss}} \text{ion loss}$$

The anionic bases A^- and B^- thus formed are stored in the ICR cell for times as long as 2 s to allow for establishment of the proton transfer equilibrium, reaction 8. The equilibrium constant K for this reaction is

$$K = \frac{[B^-][AH]}{[A^-][BH]} = \frac{k_1}{k_{-1}} \quad (10)$$

where brackets indicate the number density of the reactant species. For the neutral molecules, the number density is typically 10^{11} particles/cm^3, as measured by a Bayard-Alpert ionization gauge which has been calibrated with a Baratron type 145-AHS capacitance manometer. For the negative ions, the number density is typically 10^4 to 10^6 particles/cm^3, as measured with a capacitance bridge detector connected to the upper and lower plates of the ICR cell.[17] Ions of a particular *m/e* are detected by an RF pulse of frequency ω_1 which is applied to the upper plate of the ICR cell by the capacitance bridge detector. When ω_1 is the same as the cyclotron frequency of an ion, $\omega = qB/m$, the ion is accelerated to higher translational energy. Coherent motion of the accelerated ions induces image currents at frequency ω in the lower plate of the ICR cell, and the image currents are amplified and detected.

Finally, after about 100 collisions per ion, the concentrations of A^- and B^- begin to decrease due to diffusional losses to the upper and lower plates of the ICR cell. This process is modeled by reaction 9, a bimolecular loss channel involving ions and any neutral species M. It is very important that the rates for ion loss be much slower than the rate for establishment of the proton transfer equilibrium. We have developed a random walk model for ion losses which shows that the ions are able to diffuse slowly perpendicular to the magnetic field until they collide with the metal plates of the ICR cell and are neutralized.[18] The rate for ion loss is proportional to the total pressure M and inversely proportional to the *square* of the magnetic field strength. Therefore, the magnetic field strength is kept as high as possible to minimize the perturbation of equilibrium caused by reactions 9. Generally this condition can be satisfied because $k_1 \geq 10^{-10}$ cm^3/molecule-s for exothermic proton transfer reactions involving *n*-donor bases, compared with $k_{loss} \cong 10^{-12}$ cm^3/molecule-s for ion losses. However, some ion-molecule reactions, especially those involving carbon acids, are so slow that ion losses dominate Scheme I and cause great error in the measurement of K.[19]

Equilibrium can also be perturbed by side reactions. Clustering of ions with neutrals to form proton bound dimers occurs significantly even at 1×10^{-6} Torr for alcohols with large alkyl groups. This problem was minimized by keeping the pressure in the low 10^{-7} Torr range and trapping the ions for a longer time. Another problem is that methyl nitrite, the source of CH_3O^-, is reactive toward many anions. It can be either deprotonated to give an M − 1 anion (*m/e* 60$^-$) or undergo nucleophilic displacement to give NO_2^- (*m/e* 46$^-$). For this reason, only the minimum necessary pressure of methyl nitrite was used. One other source of side reactions encountered in this work is reaction of the anions with impurities produced by pyrolysis of the sample. Cold cathode discharge ion-gettering pumps are especially bad at coughing up impurities (for example, alkanethiols decompose to H_2S and alcohols dehydrogenate to aldehydes). Pyrolysis products can also be produced on the hot filament of the Bayard-Alpert ionization gauge. These problems were countered by turning off the ionization gauge after the pressures had stabilized and by only using liquid nitrogen trapped oil diffusion pumps on the vacuum system.

In the negative ion mode, the ICR cell also traps electrons which are scattered during the electron beam pulse. Too many electrons in the cell can cause the space charge to increase so much that plasma oscillations distort the detected ion signals and increase the rate of ion loss from the cell. The trapped electrons are easily removed by using axial resonance ejection.[20] Under normal conditions, a 5-ms pulsed RF signal at 8 MHz and 10 mV amplitude applied to the side plates is sufficient to remove the trapped electrons.

Calculation of $\delta\Delta G°_{acid}$ from K for reaction 4 requires knowing the temperature of the ions and neutral molecules in the ICR cell. Neutral molecules typically spend 1 s in the ICR vacuum system and suffer about 10^4 collisions/particle with the walls of the vacuum system before being removed by the oil diffusion pumps. This certainly is sufficient for equilibration at the temperature of the walls of the vacuum system. By connecting thermocouples to various parts of the ICR cell, we have observed increases in the temperature of the ICR cell as the current to the electron beam filament is increased. The temperature of the cell plates increases approximately as the square of the current supplied to the filament. This confirms the observations of Wren and Bowers.[21] Unfortunately, this effect causes thermal gradients in the vacuum system since the main walls are at ambient temperature, about 300 K, while the plates of the ICR cell are warmed by 15–20 °C. Temperature gradients of this magnitude are hardly noticeable in calculating $\delta\Delta G°_{acid} = -RT \ln K$ when K is in the directly measureable range of 1–200. However, the effect is significant (about 7%) over the 30 kcal/mol scale reported here. For this reason, the temperature of the neutral molecules was taken to be the average of the measured temperatures for the two side plates of the ICR cell. Usually, T was about 320 ± 5 K. The temperature of the ions must also be known, and special care must be taken because their translational energy can be altered by electric fields in the ICR cell. In the Discussion section several mechanisms are presented which we believe are effective in thermalizing the ions to a temperature very similar to that of the neutral molecules in the system.

Most compounds were obtained commercially and checked for purity (>99%) by VPC and their ICR mass spectrum. Each sample was subjected to several freeze-pump-thaw cycles on the ICR inlet system to remove entrapped impurities. The oximes were synthesized by the method of Pearson and Bruton[22] and were recrystallized from pentane, then sublimed. The alcohols *t*-BuCH(OH)R, R = Me, Et, and *i*-Pr, were obtained by reaction of the appropriate aldehyde with *tert*-butylmagnesium bromide.[23] We thank E. M. Arnett for the sample of di-*tert*-butylcarbinol. Acetylene was synthesized by dropwise addition of distilled water to calcium carbide and was collected by passing through two calcium chloride drying tubes into an evacuated sample bulb. Methyl nitrite was synthesized by dropwise addition of 2 M sulfuric acid to a 2:1 mixture (by weight) of sodium nitrite and methanol. A reservoir of methyl nitrite was wrapped in aluminum foil and stored in a freezer to retard its decomposition.

Results

Scale of Relative Acidities in the Gas Phase. Typical pulsed ICR data for the negative ion-molecule reactions in a 1:3.8:14.7 mixture of methyl nitrite, neopentyl alcohol, and *tert*-butyl alcohol are shown in Figure 1. During the first 10 ms of the reaction period, low energy (<0.2 eV) electrons accelerated through the ICR cell are captured by methyl nitrite to form predominently CH_3O^- (*m/e* 31$^-$).

$$CH_3ONO + e^- \rightarrow CH_3O^- + NO \quad (11)$$

This serves as a source of reactant negative ions by deprotonating *tert*-butyl alcohol to product *m/e* 73$^-$ and by deprotonating neopentyl alcohol to produce *m/e* 87$^-$.

$$CH_3O^- + (CH_3)_3COH \rightarrow (CH_3)_3CO^- + CH_3OH$$
$$CH_3O^- + (CH_3)_3CCH_2OH \rightarrow (CH_3)_3CCH_2O^- + CH_3OH \quad (12)$$

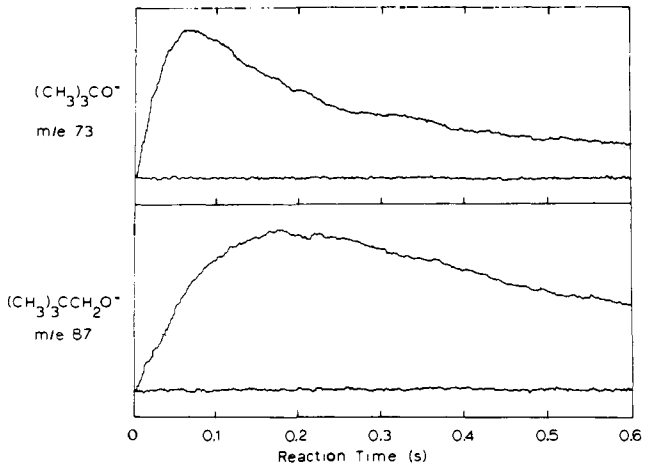

Figure 1. Raw pulsed ICR data for the abundance of $(CH_3)_3CO^-$ (*m/e* 73$^-$) and $(CH_3)_3CCH_2O^-$ (*m/e* 87$^-$) vs. reaction time. Total pressure was 2×10^{-6} Torr.

Both of these reactions are irreversible because the exothermicity is greater than 5 kcal/mol and there is negligible methanol in the system. After a certain period of reaction, the detect pulse is triggered and the capacitance bridge detector measures the abundance of the ions. By slowly varying the delay time of the detect pulse, a "time plot" of ion abundance vs. reaction time is recorded. The essential observation here is that the relative abundance of *m/e* 73$^-$ and *m/e* 87$^-$ remains constant after an initial reaction period of about 0.3 s. The approach to equilibrium is shown in Figure 2 where the ratio (*m/e* 87$^-$)/(*m/e* 73$^-$) is plotted vs. reaction time. Thermalization is quite rapid, and the relative abundances of reactants and products approach a constant value in an exponential manner, as is expected for pseudo-first-order reactions of this type. Establishment of a steady state is evidence for a reversible proton transfer between the alkoxide ions and the alcohols.

$$(CH_3)_3CO^- + (CH_3)_3CCH_2OH \rightleftharpoons (CH_3)_3CCH_2O^- + (CH_3)_3COH \quad (13)$$

The equilibrium constant for this reaction

$$K = \frac{[m/e\ 87^-][(CH_3)_3COH]}{[m/e\ 73^-][(CH_3)_3CCH_2OH]} \quad (14)$$

is a quantitative measure of the relative acidity of *tert*-butyl alcohol and neopentyl alcohol in the gas phase.

Equilibrium constants measured in this way can be used to calculate standard Gibb's free energy changes $\delta\Delta G^\circ_{acid} = -RT \ln K$ at the particular temperature T of the ICR experiment. In order to obtain a consistent scale of gas-phase acidities at 298 K, the entropy change for each equilibrium reaction is estimated and $\delta\Delta G^\circ_{acid}$ (298 K) is calculated using the expressions

$$\delta\Delta G^\circ_{acid}(298\ K) = \delta\Delta G^\circ_{acid} + \delta\Delta S^\circ_{acid}(T - 298) \quad (15)$$

This procedure assumes temperature independence for the enthalpy change $\delta\Delta H^\circ_{acid}$ and the entropy change $\delta\Delta S^\circ_{acid}$ for proton transfer reactions 4, which is certainly an excellent approximation over the narrow 20–30 °C temperature range of interest. A statistical mechanistic method for estimating the entropies is presented in the next section. The size of these corrections is quite small, generally less than 0.1 kcal/mol.

Figure 3 is a relative gas-phase acidity scale at 298 K for a 29 kcal/mol range from methanol to phenol. Multiple overlaps were done to each compound to ensure internal consistency of the data. For example, $\delta\Delta G^\circ_{acid}$(298 K) from methanol to ethanol was measured directly as 3.1 kcal/mol. This compares favorably with the sum of the $\delta\Delta G^\circ_{acid}$(298 K) values determined from direct measurements of methanol vs. toluene (0.3 kcal/mol) and toluene vs. ethanol (2.7 kcal/mol). The overall internal consistency of the scale is ±0.2 kcal/mol. These proton transfer reactions can be roughly classed in three categories of reactivity: (1) rapid reactions with rate constants greater than about 4×10^{-10} cm^3/molecule-s which involve localized negative ions such as alkoxides; (2) slower reactions which involve either a localized negative ion and delocalized carbon acid, or two delocalized oxygen or nitrogen acids such as oximes and anilines; and (3) very slow reactions between two delocalized carbon acids. Reliable overlaps are obtained for the first two classes of reactions even when they differ in acidity by as much as 3 kcal/mol. However, for the third class, reliable overlaps are not obtained if the acidity difference is greater than about 1 kcal/mol because the equilibrium ion abundances are strongly perturbed by ion loss. The acidity scale reported here is constructed only with reactions which are fast enough to give reliable overlaps.

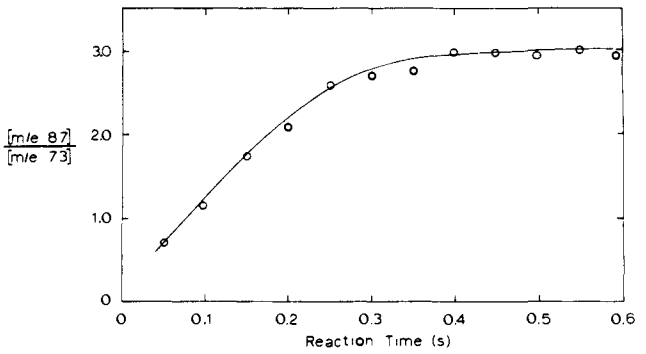

Figure 2. Time dependence of the relative abundance of two ions involved in a proton transfer equilibrium. Data from Figure 1.

Scale of Absolute Acidities. It is apparent from reaction 4 that the measured relative acidity, $\delta\Delta G^\circ_{acid}$, is equal to the difference in the absolute acidities of AH and BH. Thus

$$\delta\Delta G^\circ_{acid} = \Delta G^\circ_{acid}(BH) - \Delta G^\circ_{acid}(AH) \quad (16)$$

where ΔG°_{acid}(AH) is the standard Gibb's free energy change for the reaction

$$AH = A^- + H^+ \quad (17)$$

Absolute acidities can be calculated for many compounds from existing thermochemical data using the equation

$$\Delta G^\circ_{acid} = \Delta H^\circ_{acid} - T\Delta S^\circ_{acid} \quad (18)$$

The most generally useful method for calculating ΔH°_{acid} involves the thermochemical cycle shown in Scheme II.

Scheme II

$$AH = A\cdot + H\cdot,\ \Delta H^\circ_{298} = DH^\circ(A\text{-}H) \quad (19)$$

$$\underline{A + H = A^- + H^+,\ \Delta H^\circ_{298} \cong \Delta H^\circ_0 = IP(H) - EA(A)} \quad (20)$$

$$AH = A^- + H^+,\ \Delta H^\circ_{298} = \Delta H^\circ_{acid} \quad (21)$$

$$\Delta H^\circ_{acid} \cong DH^\circ(A\text{-}H) + IP(H) - EA(A) \quad (22)$$

Since the ionization potential of hydrogen, IP(H), is 313.6 kcal/mol[24] and a constant for all acids, the enthalpy change ΔH°_{acid} is determined by the difference between the bond strength, DH°(A–H), and the electron affinity of the radical, EA(A). A weak A–H bond and/or a high electron affinity of the radical causes molecules to be strong acids. A major limitation of this approach in the past has been the paucity of reliable EA values, but great progress has been made in the last 5 years due largely to the development of new electron photodetachment[7] and negative ion photoelectron spectroscopy experiments.[8] Another potential problem encountered with

calculations of this type is that bond dissociation energies, DH°(A–H), are usually reported at 298 K, whereas electron affinities and ionization potentials obtained from spectroscopic measurements refer to energies at 0 K. We find, however, that ΔC_p for the electron transfer reaction 20 is generally quite small due to the structural similarity of the reactants and products. For example, available thermochemical data for the reactions 23 and 24 show

$$F\cdot + H\cdot \rightarrow H^+ + F^- \quad (23)$$

$$OH\cdot + H\cdot \rightarrow H^+ + OH^- \quad (24)$$

that $\Delta H°_0 - \Delta H°_{298}$ is only 0.12 and 0.16 kcal/mol, respectively.[24] We have neglected this effect since heat capacity data are not available for the polyatomic ions encountered in this study.

Table I gives all of the $\Delta H°_{acid}$ values which can currently be calculated in this way from reported bond strengths and electron affinities. Typically the error in $\Delta H°_{acid}$ is on the order of 1–2 kcal/mol making it difficult to assign the relative acidity order for close pairs such as H_2O–propene and PH_3–HF.

Estimation of $\Delta S°_{acid}$ for use in eq 18 is done with a statistical mechanistic method similar to that of Cumming and Kebarle.[11] For reaction 17, the entropy change can be written in terms of the absolute entropies as

$$\Delta S°_{acid} = S°(A^-) + S°(H^+) - S°(AH) \quad (25)$$

The entropy of the proton[24] is well known, 26.012 eu, and the quantity $S°(A^-) - S°(AH)$ can be estimated by considering translational, electronic, vibrational, and rotational contributions. For acids of molecular weight greater than 30 amu, the translational entropies of AH and A^- are less than 0.1 eu different, so essentially cancel and can be neglected. The difference in electronic entropies of AH and A^- is also expected to be small since both the acid and its anion are isoelectronic, closed shell species. The structures of AH and A^- are usually similar enough that those vibrations less than 1000 cm^{-1} which contribute to $S°_{vib}$ at 298 K should nearly cancel. Therefore, it is rotational entropy, primarily from loss of internal rotations and symmetry changes upon proton removal, that contributes to $S°(AH) - S°(A^-)$.[11,25] Our values differ somewhat from those of Cumming and Kebarle[11] in that the entropies of the free and hindered rotors are evaluated at 298 K rather than 600 K, and the motion about the double bond in enolates, nitronates, etc., is taken as a vibration rather than a rotation for computational purposes. Thus, for $H_2C{=}NO_2^-$, the methylene group is regarded as contributing less than 0.1 eu to $S°_{vib}(AH) - S°_{vib}(A^-)$ ($\nu > 1000$ cm^{-1}). The contribution is larger for $Me_2C{=}NO_2^-$ but is canceled by the equally increased $S°_{rot}(AH)$ for no net change from $CH_2{=}NO_2^-$.

An alternate way of approximating the entropies of the anions is to assume they are the same as the experimentally measured entropies of the isoelectronic neutral species; i.e., $S°(MeO^-) \cong S°(MeF)$.[24,26] A comparison of $\Delta S°_{acid}$ values derived from the isoelectronic approximation and the statistical mechanical method is shown in Table II. Generally the agreement between the two methods is within 1 eu.

Many of the acids in Figure 3 are also included in Table I. This allows multiple "anchor" points to be used to place the relative acidity measurements on an absolute scale. Figure 4 shows the correlation between $\Delta G°_{acid}$(298 K) calculated for the compounds in Table I and the relative acidities $\delta\Delta G°_{acid}$(298 K) in Figure 3. A weighted least-squares analysis of these data constrained to unity slope gives the result.

$$\Delta G°_{acid} = 373.4 - \delta\Delta G°_{acid} \quad (26)$$

These values for absolute acidities are summarized in Table III along with the $\Delta S°_{acid}$ values calculated using the statistical

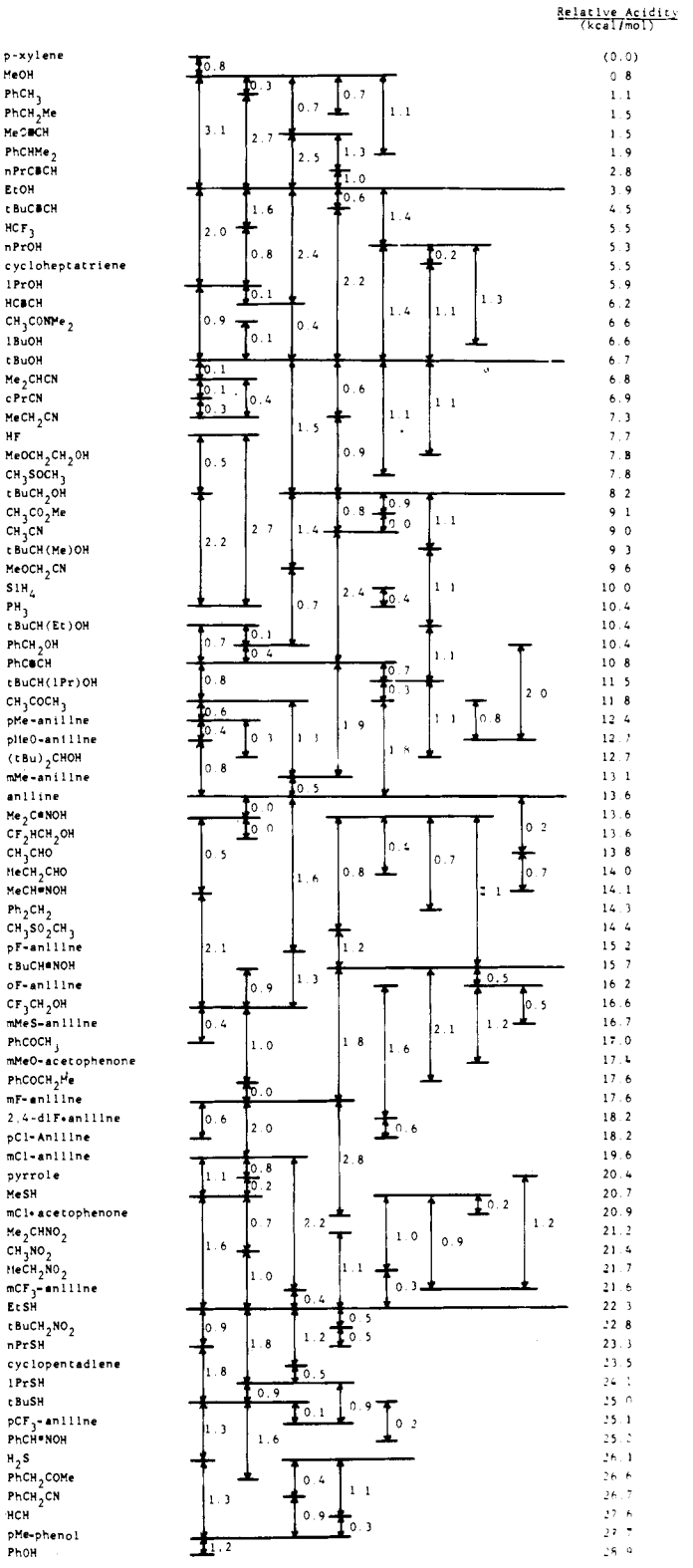

Figure 3. Relative acidity scale in the gas phase at 298 K. Each entry is $\delta\Delta G°_{acid}$ (kcal/mol) for an equilibrium of the general type $A^- + BH = B^- + AH$. Acidity increases from the top to the bottom of the scale.

mechanical method. Also shown is $\Delta H°_{acid}$, the heterolytic bond dissociation energy, which is calculated at 298 K from $\Delta G°_{acid}$ and $\Delta S°_{acid}$.

We estimate that the relative acidity measurements in Figure 3 are accurate to ±0.2 kcal/mol due to the excellent agreement of the multiple overlaps. The $\Delta S°_{acid}$ values are believed to be accurate to better than ±2 eu, or ±0.6 kcal/mol

Table I. Calculated Enthalpies for AH = A^- + H^+ at 298 K (kcal/mol)

acid	$DH°_{298}$(A–H)	ref	EA(A·)	ref	$\Delta H°_{acid}$(AH)[a]
CH_4	104.8 ± 0.3	*b*	1.84 ± 0.7	*q*	416.6 ± 1.0
H_2	104.2 ± 0.001	*b*	17.39 ± 0.5	*r*	400.4 ± 0.5
NH_3	103.2 ± 3.1	*b*	17.2 ± 0.5	*r*	399.6 ± 3.6
H_2O	119.3 ± 0.3	*b*	42.1 ± 0.05	*r*	390.8 ± 0.4
propene	86.3 ± 1.5	*cc*	12.7 ± 1.2	*t*	387.2 ± 2.7
HO·	102.3 ± 0.3	*b*	33.8 ± 0.1	*r*	382.1 ± 0.5
MeOH	104 ± 1	*d*	36.7 ± 0.9	*s*	380.9 ± 1.9
			36.2 ± 0.7	*u*	381.4 ± 1.7
$PhCH_3$	87.9 ± 1.5	*cc*	20.4 ± 1.5	*v*	381.1 ± 3.0
EtOH	104 ± 1	*d*	39.8 ± 0.7	*w*	377.8 ± 1.7
HCF_3	106 ± 1	*c*	42 ± 1.5	*r*	377.6 ± 2.5
n-PrOH	104 ± 1	*d*	41.2 ± 0.7	*w*	376.4 ± 1.7
i-PrOH	104.8 ± 1	*d*	42.4 ± 0.7	*w*	376.0 ± 1.7
t-BuOH	105.1 ± 1	*d*	43.1 ± 0.2	*s*	375.6 ± 1.2
			43.8 ± 0.7	*w*	374.9 ± 1.7
SiH_4	94 ± 2	*e*	33.2 ± 0.7	*x*	374.4 ± 2.7
t-$BuCH_2OH$	104 ± 1	*d*	44.5 ± 1.4	*s*	373.1 ± 2.4
CH_3CN	92.9 ± 2.5	*t*	34.8 ± 0.4	*t*	371.7 ± 2.9
HF	136.1 ± 0.6	*g*	78.4 ± 0.05	*r*	371.3 ± 0.7
CH_3COCH_3	98.0 ± 2.6	*h*	40.6 ± 1.3	*f*	371.0 ± 3.9
			40.5 ± 0.7	*w*	371.1 ± 3.3
PH_3	83.9 ± 3	*i*	28.9 ± 0.7	*r*	368.6 ± 3.1
MeSH	91.8 ± 2	*j*	42.9 ± 0.1	*y*	362,5 ± 2.1
	87 ± 2	*k*			357.7 ± 2.1
GeH_4	87.2 ± 2	*l*	40.1 ± 0.9	*x*	360.7 ± 2.9
EtSH	87 ± 2	*k*	45.1 ± 0.1	*y*	355.5 ± 2.1
n-PrSH	87 ± 2	*k*	46.6 ± 0.5	*y*	354.0 ± 2.5
i-PrSH	87 ± 2	*k*	46.9 ± 1.0	*y*	353.7 ± 3.0
t-BuSH	87 ± 2	*k*	47.4 ± 1.0	*y*	353.2 ± 3.0
cyclopentadiene	81.2 ± 1.2	*m*	≤42.4 ± 0.7	*z*	352.4 ± 1.9
			41.2 ± 0.5	*aa*	353.6 ± 1.7
H_2S	91.6 ± 4	*n*	53.5 ± 0.2	*r*	351.7 ± 4.2
HO_2·	47.1 ± 2.0	*n*	10.1 ± 0.2	*r*	350.6 ± 2.2
HCN	123.8 ± 2	*n*	88.1 ± 0.4	*r*	349.3 ± 2.4
PhOH	86.5 ± 2	*o*	54.4 ± 1.4	*bb*	345.7 ± 3.4
H_2Se	76 ± 4	*p*	50.9 ± 0.7	*r*	338.7 ± 5
PhSH	82.2 ± 2	*j*	56.9 ± 1.4	*bb*	338.9 ± 3.4
HCl	103.1 ± 0.2	*n*	83.4 ± 0.07	*r*	333.3 ± 0.3
HBr	87.6 ± 0.2	*n*	77.6 ± 0.07	*r*	323.6 ± 0.3
HI	71.3 ± 0.1	*n*	70.6 ± 0.07	*r*	314.3 ± 0.2

[a] $\Delta H°_{acid}(AH) = DH°_{298}(A-H) - EA(A) + 313.6$. [b] Ref 24. [c] D. M. Golden and S. W. Benson, *Chem. Rev.*, **69**, 125 (1969). [d] Ref 27. [e] W. C. Steele, L. D. Nichols, and F. G. A. Stone, *J. Am. Chem. Soc.*, **84**, 4441 (1962). [f] Ref 7a. [g] Ref 24. [h] R. K. Solly, D. M. Golden, and S. W. Benson, *Int. J. Chem. Kinet.*, **2**, 11 (1970). [i] T. McAllister and F. P. Lossing, *J. Phys. Chem.*, **73**, 2996 (1968). [j] Ref 28. [k] Ref 29. [l] B. D. Darwent, "Bond Dissociation Energies in Simple Molecules", NSRDS-NBS31 U.S. Government Printing Office, Washington, D.C., 1970. [m] S. Furuyama, D. M. Golden, and S. W. Benson, *Int. J. Chem. Kinet.*, **3**, 1237 (1971). [n] Ref 24. [o] A. J. Colussi, F. Zabel, and S. W. Benson, *Int. J. Chem. Kinet.*, **9**, 161 (1977). [p] D. A. Dixon, D. Holtz, and J. L. Beauchamp, *Inorg. Chem.*, **11**, 960 (1972). [q] G. B. Ellison, P. C. Engelking, and W. C. Lineberger, *J. Am. Chem. Soc.*, **100**, 2556 (1978). [r] Ref 1b. [s] Ref 7b. [t] A. H. Zimmerman and J. I. Brauman, *J. Am. Chem. Soc.*, **99**, 3565 (1977). [u] P. C. Engelking, G. B. Ellison, and W. C. Lineberger, *J. Chem. Phys.*, **69**, 1826 (1978). [v] J. H. Richardson, L. M. Stephenson, and J. I. Brauman, *J. Chem. Phys.*, **63**, 74 (1975). [w] G. B. Ellison, private communication. [x] K. J. Reed and J. I. Brauman, *J. Chem. Phys.*, **61**, 4380 (1974). [y] B. K. Janousek and J. I. Brauman, private communication. [z] J. H. Richardson, L. M. Stephenson, and J. I. Brauman, *J. Chem. Phys.*, **59**, 5068 (1973). [aa] P. C. Engelking and W. C. Lineberger, *J. Chem. Phys.*, **67**, 1412 (1977). [bb] J. H. Richardson, L. M. Stephenson, and J. I. Brauman, *J. Am. Chem. Soc.*, **97**, 2967 (1975). [cc] M. Rossi and D. M. Golden, *J. Am. Chem. Soc.*, **101**, 1230 (1979).

in $T\Delta S°$. Finally, the excellent correlation between the several anchor points and the relative acidity scale precludes any major systematic accumulation of errors and leads to an estimated uncertainty of ±2 kcal/mol in $\Delta H°_{acid}$ and $\Delta G°_{acid}$ values shown in Table III.

Calculated $\Delta H°_{acid}$ values from Table I are compared in Table IV with the ICR determinations shown in Table III. Generally the agreement is acceptable, but a few consistent trends are worth noting. First, the aliphatic alcohols and acetone have calculated $\Delta H°_{acid}$ values about 2 kcal/mol greater than the ICR determinations. According to eq 22, this implies that either the reported bond strengths are too large or the reported electron affinities are too small. Since the reported bond strengths were determined by measuring activation energies for radical producing decomposition reactions, they may be too large due to a small activation energy barrier for radical–radical recombination.[27] It is also apparent that there is a large difference between the $\Delta H°_{acid}$ values for phenol (−5.7 kcal/mol). This suggests a much lower O–H bond strength in phenol or higher electron affinity for the phenoxy radical. Most likely the electron affinity for C_6H_5O· is closer to 48.7 kcal/mol than the reported electron photodetachment value of 54.4 kcal/mol. A discrepancy is also apparent for methanethiol. The ICR data suggest an average RS–H bond strength of 88.6 kcal/mol, compared with literature values of 87 kcal/mol[28] and 91.8 kcal/mol.[29]

Derived Thermochemical Data. The enthalpy change $\Delta H°_{acid}$ for reaction 5 can be expressed as the heats of formation of the products less that of the reactant.

$$\Delta H°_{acid} = \Delta H°_f(A^-) + \Delta H°_f(H^+) - \Delta H°_f(AH) \quad (27)$$

If $\Delta H°_f(AH)$ is known, then the data in Table III can be used

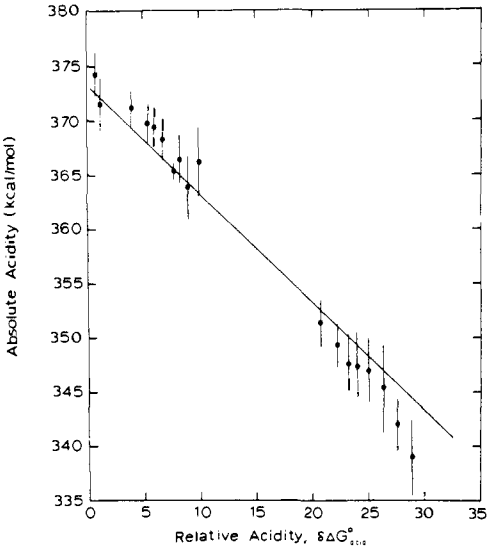

Figure 4. Comparison between ΔG°_{acid} for AH = A^- + H^+ calculated from bond strengths and electron affinities (Table I) and relative acidities $\delta\Delta G^\circ_{acid}$ determined from pulsed ICR equilibria (Figure 3).

Table II. Comparison of ΔS°_{acid} Values Derived from the Isoelectronic Approximation and from Statistical Mechanical Calculations[a]

acid	ΔS°_{acid}(iso)[b]	ΔS°_{acid} (stat mec)	difference
CH_3OH	22.0	22.1	−0.1
CH_3CH_2OH	21.8	22.0	−0.2
PhOH	23.3	23.0	−0.3
CH_3SH	21.0	21.3	−0.3
CH_3CH_2SH	21.3	21.0	0.3
PhSH	20.7	20.9	−0.2
$PhCH_3$	25.8	22.4	3.2
$PhNH_2$	24.7	24.4	0.3
HCF_3	26.3	26.0	−0.3
HCCH	26.3	27.2	−0.9
CH_3CCH	25.4	26.0	−0.6
PhCCH	26.1	26.0	−0.1
CH_3NO_2	23.7	22.4	−1.3
CH_3CN	25.1	26.3[c]	−1.2
CH_3CHO	23.2	22.8	0.4

[a] In cal/mol-deg for the process AH = A^- + H^+. [b] Equation 25, using the entropy of the isoelectronic neutral as an approximation to $S^\circ(A^-)$. [c] External rotations used, with ketene as the model for the anion.

to calculate the heat of formation of the anion by taking $\Delta H^\circ_{f,298}(H^+)$ = 367.186 kcal/mol.[24] Derived heats of formation of anions are given in column 6 of Table III for those acids with reasonably reliable heats of formation.

For many of the compounds in Table III, either a bond strength or an electron affinity has been determined previously. Table V shows how these data can be used in eq 22 to calculate the other quantity. The ΔH°_{acid} values are taken from Table III. It is apparent that the α-C–H bond strength in aldehydes is considerably weaker than in ketones and esters. Furthermore, α-methyl substitution in aldehydes lowers the C–H bond strength. In pyrrole the N–H bond strength at 102.2 kcal/mol is considerably stronger than the C–H bond in cyclopentadiene at 81.2 ± 1.2 kcal/mol. This is opposite to the general trend for secondary N–H bonds to be *weaker* than the structurally similar C–H bonds. A five-electron delocalized π system can be written for cyclopentadienyl, but delocalization in the pyrrolyl system is not favored. It would replace a six-electron π system with a nonaromatic five-electron one.

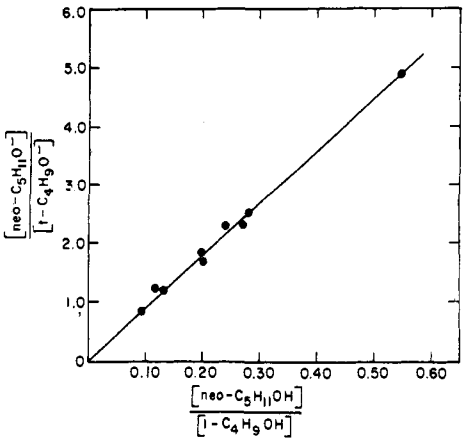

Figure 5. Variation of relative abundance of anions as partial pressure of the neutral acids is changed. Slope of the plot is the equilibrium constant for proton transfer, as is shown in eq 28.

Table V also shows electron affinities calculated from literature bond strengths and ICR determinations of ΔH°_{acid}. The results show a pronounced decrease in EA for α-methyl substitution onto a variety of carbon radicals such as benzyl and cyanomethylene. This is consistent with the previously reported α-methyl effects in carbonyl radicals. The EA's for the series $PhCH_2$·, PhNH·, and PhO· increase with increasing electronegativity of the formally anionic atom. The effect is not linear with electronegativity due to differing amount of delocalization into the ring for the radical and anion of each. The derived EA of cycloheptatrienyl at 13.1 ± 4 kcal/mol is considerably lower than that of cyclopentadienyl (Table I) at 42 kcal/mol. The comparable sizes of the EA's for cycloheptatrienyl and allyl, however, can be taken as evidence for reduced delocalization of charge in $C_7H_7^-$ due to ring puckering.

Discussion

Experimental Tests for Attainment of Equilibrium. Data such as in Figure 1 show that a steady-state condition is reached in the ICR cell, but additional tests are needed to demonstrate that the system of ions and neutral molecules reaches a well defined thermal, or closely thermal, state. Such a condition must be satisfied in order for the thermochemical results of the experiments to be reliable and meaningful.

A number of additional experiments were performed to test if equilibrium is attained for these proton-transfer reactions. The measured equilibrium constant, eq 10, should be independent of variations in the relative pressure of the neutral acids. This is demonstrated in Figure 5 for the two acids *tert*-butyl alcohol and neopentyl alcohol. Rearrangement of the expression for the equilibrium constant gives

$$\frac{[m/e\ 87^-]}{[m/e\ 73^-]} = K\frac{[(CH_3)_3CCH_2OH]}{[(CH_3)_3COH]} \qquad (28)$$

As the partial pressures of two alcohols is varied, the equilibrium abundance of *tert*-butoxide, *m/e* 73⁻, and neopentoxide, *m/e* 87⁻, should adjust accordingly in order to maintain a constant value of K. Figure 5 shows a plot of this type for reaction 13 and gives a value of 9.0 ± 0.5 for the equilibrium constant.

It is essential that the interconversion of reactants and products be rapid compared with the time scale of the experiment. In pulsed ICR studies this can be readily demonstrated by using the pulsed double resonance ejection technique. Figure 6 shows a double resonance ejection experiment for reaction

Table III. Thermochemical Data from Pulsed ICR Equilibria

acid	$\Delta S°_{acid}$[a]	$\Delta H°_{acid}$[b]	$\Delta G°_{acid}$(298 K)[c]	$\Delta H°_{f,298}$(AH)[d]	$\Delta H°_{f,298}(A^-)$[e]
MeOH	22.0	379.2	372.6	−48.0	−36.0
EtOH	22.0	376.1	369.5	−56.2	−47.5
n-PrOH	22.0	374.7	368.1	−61.3	−53.8
i-PrOH	22.0	374.1	367.5	−65.2	−58.3
i-BuOH	22.0	373.4	366.8	−67.9	−61.7
t-BuOH	22.0	373.3	366.7	−74.7	−68.6
$MeO(CH_2)_2OH$	23.2	372.5	365.6	−87.4	−82.1
t-$BuCH_2OH$	22.0	371.8	365.2	−76.1[g]	−71.5
t-BuCH(Me)OH	22.0	370.7	364.1	−83.8[g]	−80.3
t-BuCH(Et)OH	22.0	369.6	363.0	−88.7[g]	−86.3
$PhCH_2OH$	22.0	369.6	363.0	−22.5	−20.1
t-BuCH(*i*-Pr)OH	22.0	368.5	361.9	−93.6[g]	−92.3
$(t\text{-Bu})_2CHOH$	22.0	367.3	360.7	−99.1[g]	−99.0
CHF_2CH_2OH	24.0	367.0	359.8	−148.3[g]	−148.5
CF_3CH_2OH	25.5	364.4	356.8	−207.0[g]	−209.8
PhOH	23.0	351.4	344.5	−23.0	−38.8
p-Me-phenol	23.0	352.6	345.7	−30.0	−44.6
$Me_2C{=}NOH$	23.2	366.7	359.8	−13.0[g]	−13.5
$MeCH{=}NOH$	23.2	366.2	359.3	−4.7	−5.7
t-$BuCH{=}NOH$	23.2	364.6	357.7	−23.2[g]	−25.8
$PhCH{=}NOH$	23.2	355.1	348.2	25.8	13.7
MeSH	21.0	359.0	352.7	−5.5	−13.7
EtSH	21.0	357.4	351.1	−11.0	−20.8
n-PrSH	21.0	356.4	350.1	−16.1	−26.9
i-PrSH	21.0	355.6	349.3	−18.2	−29.8
t-BuSH	21.0	354.7	348.4	−26.1	−38.6
H_2S	21.3	353.4	347.1	−4.8	−18.5
HF	19.3	371.5	365.7	−64.8	−60.5
HCF_3	26.0	375.6	367.9	−165.7	−157.2
SiH_4	27.1	371.5	363.4	8.2	12.5
PH_3	24.9	370.4	363.0	1.3	4.5
HCN	24.6	353.1	345.8	32.3	18.2
$MeC{\equiv}CH$	26.0	379.6	371.9	44.3	56.8
n-$PrC{\equiv}CH$	26.0	378.3	370.6	34.5	45.7
t-$BuC{\equiv}CH$	26.0	376.6	368.9	25.1[g]	34.6
$HC{\equiv}CH$	27.4	375.4	367.2	54.3	62.5
$PhC{\equiv}CH$	26.0	370.3	362.6	78.3	81.5
cyclopentadiene	20.8	356.1	349.9	32.4	21.3
pyrrole	26.0	360.7	353.0	25.9	19.5
cycloheptatriene	20.1	373.9	367.9	44.5	51.2
anilines					
pMe	24.1	368.2	361.0	12.9[g]	13.9
p-MeO	24.0	367.9	360.7		
m-Me	24.4	367.6	360.3	12.9[g]	13.3
H	24.4	367.1	359.8	20.8	20.7
p-F	24.4	365.5	358.2		
o-F	24.4[f]	364.5[h]	357.2[h]		
m-MeS	24.4	364.0	356.7	24.8[g]	21.6
m-F	24.4	363.1	355.8	−25.3[g]	−29.4
2,4-diF	24.4[f]	362.5[h]	355.2[h]		
p-Cl	24.4	362.5	355.2		
m-Cl	24.4	361.1	353.8	13.7[g]	7.6
m-CF_3	24.4	359.1	351.8	−139.7[g]	−147.8
p-CF_3	24.5	355.6	348.3		
$PhCH_3$	22.4	379.0	372.3	12.0	23.8
$PhCH_2Me$	21.6	378.3	371.9	7.1	18.3
$PhCH(Me)_2$	20.2	377.5	371.5	1.0	11.3
p-xylene	23.8	380.5	373.4	4.3	17.6
Ph_2CH_2	18[f]	364.5[h]	359.1[h]		
CH_3CN	26.3	372.2	364.4	19.0	24.1
$MeCH_2CN$	25.5	373.7	366.1	12.3	18.8
$(Me)_2CHCN$	24.2	373.8	366.6	5.6	12.2
c-PrCN	25.5	374.1	366.5	43.5[g]	50.4
$MeOCH_2CN$	25.5	371.4	363.8	−12.5[g]	−8.3
$PhCH_2CN$	22[f]	353.3[h]	346.7[h]		
CH_3CHO	22.8	366.4	359.6	−39.7	−40.5
$MeCH_2CHO$	21.9	365.9	359.4	−45.5	−46.8

Table III (*Continued*)

acid	$\Delta S°_{acid}$[a]	$\Delta H°_{acid}$[b]	$\Delta G°_{acid}$(298 K)[c]	$\Delta H°_{f,298}$(AH)[d]	$\Delta H°_{f,298}(A^-)$[e]
CH_3COCH_3	24.0	368.8	361.6	−51.7	−50.1
$PhCOCH_3$	22.8	363.2	356.4	−22.0	−26.0
m-MeO acetophenone	22.8	362.8	356.0	−59.8[g]	−64.2
m-Cl acetophenone	22.8	359.3	352.5	−29.1[g]	−37.0
$PhCOCH_2Me$	22.0	362.4	355.8	−26.0	−30.8
$PhCH_2COMe$	19[f]	352.5[h]	346.8[h]	−24.9[g]	−39.6[h]
CH_3CONMe_2	22.6[f]	373.5[h]	366.8[h]		
CH_3SOCH_3	23.7	372.7	365.6	−34.6	−29.1
CH_3CO_2Me	22.6[f]	371.0[h]	364.3[h]	−98.0	−94.2[h]
$CH_3SO_2CH_3$	25.4	366.6	359.0	−89.1	−89.7
CH_3NO_2	22.4	358.7	352.0	−17.9	−26.4
$MeCH_2NO_2$	21.6	358.1	351.7	−23.8	−32.8
Me_2CHNO_2	20.2	358.2	352.2	−33.9	−42.9
t-$BuCH_2NO_2$	21.6	357.0	350.6	−45.2[g]	−55.3

[a] Entropy change for the process AH = A^- + H^+; ±2 cal/mol-deg unless stated otherwise. [b] Enthalpy change for the process AH = A^- + H^+; ±2 kcal/mol. [c] $\Delta H°_{acid} - 0.298\Delta S°_{acid}$, kcal/mol. [d] Heats of formation from references 26 and 38. [e] Calculated using eq 27; ±3 kcal/mol except where noted. [f] ±5 cal/mol-deg; due to uncertainty in V_0 or $S°_f$; see text. [g] Estimated by Group Additivity methods, reference 26. [h] ±4 kcal/mol, due to uncertainty in $\Delta S°_{acid}$.

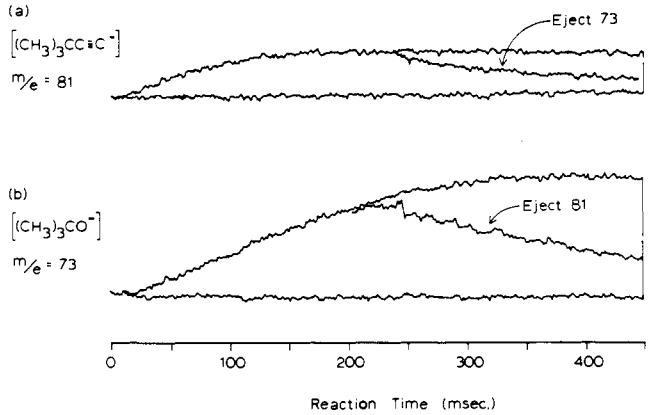

Figure 6. Pulsed double resonance ejection time plots: (a) abundance of *m/e* 81$^-$ vs. time with ejection of *m/e* 73$^-$ beginning at 250 ms, and (b) abundance of *m/e* 73$^-$ vs. time with ejection of *m/e* 81$^-$ beginning at 250 ms. See reaction 29.

in *tert*-butyl alcohol and 3,3-dimethyl-1-butyne.

$$(CH_3)_3CC{\equiv}C^- + (CH_3)_3COH \quad (m/e\ 81^-)$$
$$\underset{k_{-1}}{\overset{k_1}{\rightleftharpoons}} (CH_3)_3CO^- + (CH_3)_3CC{\equiv}CH \quad (m/e\ 73^-) \qquad (29)$$

The upper part of the trace in Figure 6a is a standard ICR time plot of *m/e* 81$^-$ which shows equilibrium after about 300 ms. The lower part of the trace in Figure 6a shows how the abundance of $(CH_3)_3CC{\equiv}C^-$ is decreased when $(CH_3)_3CO^-$ is ejected from the ICR cell by pulsed double resonance ejection beginning at a delay time of 250 ms. The rate of decay of $(CH_3)_3CC{\equiv}C^-$ is equal to $k_1[(CH_3)_3COH]$, the product of the forward rate constant and the number density of *tert*-butyl alcohol. Similarly, the upper part of the trace in Figure 6b is a standard time plot of *m/e* 73$^-$ which levels out after about 300 ms, and the lower part of the trace shows that the abundance of $(CH_3)_3CO^-$ decreases when the system is perturbed by ejection of *m/e* 81$^-$. Double resonance ejection experiments are performed routinely on every new reaction system to test whether the ionic species are rapidly interconverting. If ejection of an ion does not change the abundance of another ionic species in the trap, then the two species are not coupled by a rapid chemical reaction and the equilibrium constant cannot be measured.

Table IV. $\Delta H°_{acid}$ for AH = A + H. Comparison of Calculated Values from Table I with ICR Determinations from Table III

acid	$\Delta H°_{acid}$ (Table I)	$\Delta H°_{acid}$ (Table III)	difference
MeOH	380.9 ± 1.7	379.2	1.7
	381.4 ± 1.7		2.2
EtOH	377.8 ± 1.7	376.1	1.7
n-PrOH	376.4 ± 1.7	374.7	1.7
i-PrOH	376.0 ± 1.7	374.1	1.9
t-BuOH	375.6 ± 1.2	373.3	2.3
	374.9 ± 1.7		1.6
t-$BuCH_2OH$	373.1 ± 2.4	371.8	1.3
PhOH	345.7 ± 3.4	351.4	−5.7
MeSH	362.5 ± 2.1	359.0	3.5
	357.7 ± 2.1		−1.3
EtSH	355.5 ± 2.1	357.4	−1.9
n-PrSH	354.0 ± 2.5	356.4	−2.4
i-PrSH	353.7 ± 3.0	355.6	−1.9
t-BuSH	353.2 ± 3.0	354.7	−1.5
H_2S	351.7 ± 4.2	353.4	−1.7
HF	371.3 ± 0.7	371.5	−0.2
HCF_3	377.6 ± 2.5	375.6	2.0
SiH_4	374.4 ± 2.7	371.5	2.9
PH_3	368.6 ± 3.1	370.4	−1.8
HCN	349.3 ± 2.4	353.1	−3.8
cyclopentadiene	352.4 ± 1.9	356.1	−3.7
	353.6 ± 1.7		−2.5
$PhCH_3$	378.2 ± 2.5	379.0	−0.8
CH_3CN	371.7 ± 2.9	372.2	−0.5
CH_3COCH_3	371.0 ± 3.9	368.8	2.2
	371.1 ± 3.3		2.5

The multiple overlaps shown in Figure 3 demonstrate that the measured $\Delta G°_{acid}$ values are state properties independent of path. Such agreement is evidence that thermalization is occurring. Consider three separate experiments linking three species:

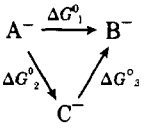

If the $\Delta G°$ linking A^- to B^- agrees with the sum linking A^- to C^- and C^- to B^-, then there are only two possible conclusions: (1) the species A^-, B^-, and C^- are in the same energy states in each of the three experiments, or (2) if excited species are involved in one or more of the experiments, the equilibrium constants are relatively insensitive to such states of excitation.

Table V. Bond Strengths and Electron Affinities Calculated from ICR Data

acid	$\Delta H°_{acid}$ (Table III)	lit. values DH°(A-H)	lit. values EA(A)	ref	calcd values; eq 22 DH°(A-H)	calcd values; eq 22 EA(A)
p-xylene	380.5	84.8 ± 2		*a*		17.9 ± 4
$PhCH_2Me$	378.3	78 ± 2		*a*		13.3 ± 4
HC≡CH	375.4	128 ± 2		*b*		66.2 ± 4
		115 ± 7		*a*		53.2 ± 9
cycloheptatriene	373.9	73.4 ± 2		*a*		13.1 ± 4
Me_2CHCN	373.8	82.5 ± 1		*a*		22.3 ± 3
CH_3CO_2Me	371.0		43.5 ± 1.4	*d*	100.9 ± 3.4	
$PhNH_2$	367.1	80 ± 3		*a*		26.5 ± 5
CH_3CHO	366.4		41.7 ± 1.4	*d*	94.5 ± 3.4	
$MeCH_2CHO$	365.9		38.9 ± 1.2	*d*	91.2 ± 3.2	
$PhCOCH_3$	363.2		47.6 ± 1.8	*d*	97.2 ± 3.8	
pyrrole	360.7		55.1 ± 0.3	*e*	102.2 ± 2.3	

[a] J. A. Kerr, *Chem. Rev.*, **66**, 465 (1966). [b] D. K. Sen Sharma and J. L. Franklin, *J. Am. Chem. Soc.*, **95**, 6562 (1973). [c] K. W. Egger and A. T. Cocks, *Helv. Chim. Acta.*, **56**, 1517 (1973). [d] Ref 7a. [e] J. H. Richardson, L. M. Stephenson, and J. I. Brauman, *J. Am. Chem. Soc.*, **97**, 1160 (1975).

Numerous studies have shown that the rate and equilibrium constants for ion-molecule reactions are affected by excess energy. It seems reasonable then to choose conclusion (1) as the more likely explanation for the consistency of the overlapping checks shown in Figure 3.

The final, and perhaps most convincing, evidence for the validity of the experimental ICR data concerns the excellent agreement shown in Figure 4 between the ICR data and the $\Delta G°_{acid}$ values calculated from available bond strengths and electron affinities. Such agreement would not be expected over a 30 kcal/mol range if the experiment suffered from inherent systematic errors.

Tests such as these have also been performed for a wide variety of positive ion proton transfer reactions.[4] Proving the attainment of thermal equilibrium is difficult in any gas-phase experiment involving reactive systems, and certainly no single experimental technique can be expected to work under all conditions for all types of reactions. However, strong evidence is available now that thermal or closely thermal ions are produced in pulsed ICR experiments after the ions have suffered 10 to 30 collisions/particle, and the technique seems to work very well for bimolecular reactions with rate constants greater than about 1×10^{-12} cm^3/molecule-s.

Mechanisms for Thermalization of Ions. When negative ions are produced, as in reaction 6, the anion base X^- may have excess internal energy due to the electron impact process and excess translational energy due to the presence of electrostatic fields inside the ICR cell. The excess energies are not large because in this work the anion base CH_3O^- is produced by low energy (less than 1 eV) electron impact on methyl nitrite and the depth of the electrostatic trapping well is typically only 0.7 V. However, some of this excess energy may be transferred to the reactants of interest in reaction 7 when the anion base deprotonates the two acids. In addition, the exothermicity of reaction 7 (up to 29 kcal/mol for the case of CH_3O^- plus phenol) can also be deposited in the ions to produce excited ions $(A^-)^*$.

Scheme III shows several mechanisms which are efficient in removing excess energy from the ions and thermalizing them at the temperature of the neutral molecules in the ICR cell.

Scheme III

collisional deactivation

$$(A^-)^* + M \rightarrow A^- + M^* \quad (30)$$

proton exchange

$$(A^-)^* + AH \rightarrow [A^- \cdots H^+ \cdots A^-]^* \rightarrow A^- + AH^* \quad (31)$$

spontaneous emission

$$(A^-)^* \rightarrow A^- + h\nu \quad (32)$$

Relaxation of excess translational momentum in the ion can occur by a nonspecific deactivation mechanism such as reaction 30. The efficiency of this process depends on the relative mass of A^- and molecule M, but generally about 10 collisions are sufficient. In the ICR cell, ions are formed initially with excess translational energy due to the electrostatic trapping well parallel to the magnetic field.[30] However, ions quickly relax to the center of the ICR cell and the bottom of the trapping well as a result of momentum relaxing collisions such as reaction 30. Since experiments are always carried out under conditions where the number density of ions is far less than the number density of neutral molecules, excess energy transferred to the neutral molecules never finds its way back into the ions.

Reaction 31, near resonant proton transfer, is an efficient mechanism in these systems for relaxation of excess internal energy in the ions.[31] Since the hydrogen bonded intermediates $(A\cdots H\cdots A)^-$ live for a long time and can be collisionally stabilized as cluster ions, it is likely that some of the excess internal energy in the ions is transferred to the neutral molecule as the complex breaks up.

The final process shown in Scheme III, spontaneous emission, is a likely possibility for the pulsed ICR experiments because the ions are trapped typically for 1 s, a time comparable to the lifetime for IR emission from polyatomic molecules. Unfortunately, not much seems to be known about spontaneous emission from large polyatomic molecules, but there is indirect evidence like bimolecular formation of cluster ions and generation of stable negative ion radicals from direct capture of electrons.[10]

Structure of the Anions. No explicit information regarding the structure of ions is furnished by ICR experiments. Some rationale must be given for assuming certain structures for the M − 1 anions besides analogy to solution phase observations. The reversal of acidities in the gas phase compared with solution phase results and the uncertainty of the site of reaction within the molecule makes structure assignments difficult. However, inferences can be made which are consistent with the following experimental observations.

(1) **Alcohols and Alkanethiols.** Since these compounds are less acidic in the gas phase than expected from correlations with acidities in protic solvents,[32] it is possible that it is the proton on the α carbon, not the heteroatom, that is acidic, due to the polar effect of -OH or -SH. No M − 2 anion is observed, however, for CD_3OH or CD_3SH under typical conditions in the ICR spectrometer. In addition, ethers show no $(M - 1)^-$ peak, but rather products of displacement or elimination upon base treatment. Consequently, all M − 1 peaks for alcohols and alkanethiols are assumed to be the localized RO^- and RS^- anions.

(2) **Oximes.** The hydrogen on oxygen is the most acidic one since vinylic hydrogens are known to be of low acidity.[33] The hydrogens on the α carbon could also be acidic, in analogy to ketones; however, pivaldoxime and benzaldoxime have no such hydrogens and display acidities relative to the other oximes consistent with known substituent effects.

(3) **Anilines.** The amine hydrogens are the acidic ones. The ring protons in substituted benzenes such as chlorobenzene and trifluorotoluene are not removed by methoxide,[34] and the $-NH_2$ group should be less effective than -Cl or $-CF_3$ in stabilizing a phenyl anion. The linearity of the Hammett plot for the substituted anilines[32] further attests to this conclusion. The *m*- and *p*-toluidines could possibly be carbon acids rather than nitrogen acids. However, the Hammett σ for $-NH_2$ implies that deprotonation at the benzylic site should be less likely than for toluene, or more than 12 kcal/mol less acidic than observed.

(4) **Acetylenes.** Propyne-d_3 produces both the acetylenic M − 1 anion and the propargylic (or allenic) M − 2 anion on reaction with hydroxide.[35] The delocalized M − 2 anion rapidly reacts away to form the localized M − 1 anion so that at long times it is the acetylenic system being measured.

(5) **Toluenes.** Neither *tert*-butylbenzene nor benzene are deprotonated by hydroxide[34] so benzylic protons are more acidic than ring or β protons by at least 12 kcal/mol.

(6) **Carbonyl Compounds, Nitriles, Nitroalkanes, Sulfones, and Sulfoxides.** These acids are assumed to deprotonate on the carbon α to the electron-withdrawing group, but the site of reprotonation of the resulting ambident anion is not unequivocal. For acetaldehyde, reprotonation on oxygen would give its enol, vinyl alcohol. If one assumes that replacing a methoxy group in methyl vinyl ether with a hydroxy group has the same effect on $\Delta H°_f$ as it does in methyl ethyl ether,[26] then $\Delta H°_{f,298}(CH_2{=}CHOH) = -31.8$ kcal/mol, or 8 kcal/mol greater than for acetaldehyde. A transient neutral ICR study provides similar experimental values.[36] This represents a sizeable activation barrier to enol formation from the enolate, and effectively rules out O-protonation in this case. It is assumed other monocarbonyl compounds also reprotonate on carbon. For the oximes, carbon protonation is disfavored by 14 kcal/mol based on $\Delta H°_{f,298}$ of the nitrosoalkanes.[26] The possibility of formation of nitronic acids, ketenimines, and structures such as $CH_2{=}S(OH)CH_3$ has not been determined, though solution phase results indicate them unlikely to be favored.

Excess Energy in Fragmentation Processes. The use of appearance potentials of ions from electron impact mass spectrometry to determine heats of formation of the products only gives upper limits to these values. If the products are formed with excess energy, then the calculated $\Delta H°_f$ will be too high. It would be of interest to determine the amount of excess energy in given fragmentation products. Excess translational energy can be determined by the spreading of the ion beam in time-of-flight mass spectrometers.[37] However, this experiment yields no information on the neutral products or the amount of energy distributed in modes other than translational. For reaction 33

$$AB + e^- \rightarrow A^- + B\cdot \qquad (33)$$

the following equation can be written.

$$\Delta H°_{298}(33) = \Delta H°_{f,298}(A^-) + \Delta H°_{f,298}(B\cdot) - \Delta H°_{f,298}(AB) \qquad (34)$$

The total excess energy distributed between the products A^- and B· is

$$\Delta H°_{298}(\text{excess}) = AP(A^-) - \Delta H°_{298}(33) \qquad (35)$$

The term $\Delta H°_{298}(33)$ can be evaluated since $\Delta H_f(A^-)$ values are available from this study for selected compounds. The excess energy for some typical fragmentation reactions has been calculated and these results are tabulated in Table VI for some simple molecules. The examples are chosen for the neutral products to be as unequivocal as possible. The results indicate that more than 50% of the minimum energy required for fragmentation of these simple molecules may be in excess of the energy required to give thermal products. Of course, these calculations do not allow specification of how the excess energy is distributed in the molecules. Due to the large excess energies involved in appearance potential measurements, it would appear that thermal ion-molecule equilibria experiments would be a more accurate source of thermochemical data.

Table VI. Excess Energy in the Products of Dissociative Attachment Reactions

compd	products	AP[a]	$\Delta H°_{298}(33)$[a]	$\Delta H°_{22}(\text{excess})$[b]
MeOH	H; MeO^-	64	64	0
EtOH	H; EtO^-	60	61	0
	2H; $C_2H_3O^-$ [c]	134	119	15
CF_4	F; CF_3^-	124	85	39
$CH_2{=}CH_2$	H, H; C_2H^-	159	101	58
$(CN)_2$	CN; CN^-	101	44	57

[a] kcal/mol, ref 39. [b] Equation 35. [c] Assumed to be enolate of acetaldehyde.

Acknowledgments. We gratefully acknowledge grant support from the National Science Foundation (CHE77-10024), the National Institutes of Health (GM-23416-02), the Alfred P. Sloan Foundation, and the donors of the Petroleum Research Fund, administered by the American Chemical Society.

References and Notes

(1) (a) J. L. Franklin, J. G. Dillard, H. M. Rosenstock, J. T. Herron, K. Draxl, and F. H. Field, "Ionization Potentials, Appearance Potentials, and Heats of Formation of Gaseous Positive Ions", NSRDS-NBS-26, U.S. Government Printing Office, Washington, D.C., 1969; (b) H. M. Rosenstock, K. Draxl, B. W. Steiner, and J. T. Herron, "Energetics of Gaseous Ions", *J. Phys. Chem. Ref. Data, Suppl. No. 1, 6* (1977).
(2) (a) R. Yamdagni and P. Kebarle, *J. Am. Chem. Soc.*, **98**, 1320 (1978); (b) P. Kebarle, *Annu. Rev. Phys. Chem.*, **28**, 445 (1977).
(3) D. K. Bohme in "Interactions Between Ions and Molecules", P. Ausloos, Ed., Plenum Press, New York, 1974, p 489.
(4) (a) J. F. Wolf, R. H. Staley, I. Koppel, M. Taagepera, R. T. McIver, Jr., J. L. Beauchamp, and R. W. Taft, *J. Am. Chem. Soc.*, **99**, 5417 (1977); D. H. Aue, H. M. Webb, and M. T. Bowers, *ibid.*, **98**, 311 (1976).
(5) (a) R. W. Taft in "Proton Transfer Reactions", E. F. Caldin and V. Gold, Eds., Chapman and Hall, London, 1975, p 31; (b) D. H. Aue, H. M. Webb, and M. T. Bowers, *J. Am. Chem. Soc.*, **98**, 318 (1976).
(6) C. E. Melton, "Principles of Mass Spectroscopy and Negative Ions", Marcel Dekker, New York, 1970.
(7) (a) A. H. Zimmerman, K. J. Reed, and J. I. Brauman, *J. Am. Chem. Soc.*, **99**, 7203 (1977); (b) B. K. Janousek, A. H. Zimmerman, K. J. Reed, and J. I. Brauman, *ibid.*, **100**, 6142 (1978).
(8) W. C. Lineberger in "Chemical and Biochemical Applications of Lasers", Vol. I, C. B. Moore, Ed., Academic Press, New York, 1974.
(9) (a) S. J. Nalley, R. N. Compton, H. C. Schweinler, and V. E. Anderson, *J. Chem. Phys.*, **59**, 4125 (1973); (b) T. O. Tiernan in "Interactions Between Ions and Molecules", P. Ausloos, Ed., Plenum Press, New York, 1974, p 353.
(10) L. J. Rains, H. W. Moore, and R. T. McIver, Jr., *J. Chem. Phys.*, **68**, 3309 (1978).
(11) J. B. Cumming and P. Kebarle, *Can. J. Chem.*, **56**, 1 (1978).
(12) G. I. Mackay, R. S. Hemsworth, and D. K. Bohme, *Can. J. Chem.*, **54**, 1624 (1976).
(13) (a) J. E. Bartmess and R. T. McIver, Jr., *J. Am. Chem. Soc.*, **99**, 4163 (1977); (b) R. T. McIver, Jr., and J. S. Miller, *ibid.*, **96**, 4323 (1974); R. T. McIver, Jr., and John R. Eyler, *ibid.*, **93**, 6334 (1971).
(14) R. T. McIver, Jr., *Rev. Sci. Instrum.*, **41**, 555 (1970).
(15) (a) R. T. McIver, Jr., *Rev. Sci. Instrum.*, **49**, 111 (1978); (b) R. T. McIver, Jr., in "Ion Cyclotron Resonance Spectrometry", H. Hartmann and K.-P. Wanczek, Eds., Springer-Verlag, Berlin, 1978, p 97.
(16) K. Jager and A. Henglein, *Z. Naturforsch. A*, **22**, 700 (1967).
(17) (a) R. L. Hunter and R. T. McIver, Jr., *Chem. Phys. Lett.*, **49**, 577 (1977); (b) *Anal. Chem.*, **51**, 699 (1979).
(18) R. T. McIver, Jr., and M. B. Ruggera, to be published.
(19) W. E. Farneth and J. I. Brauman, *J. Am. Chem. Soc.*, **98**, 7891 (1976).
(20) J. L. Beauchamp and J. T. Armstrong, *Rev. Sci. Instrum.*, **40**, 123 (1969).
(21) (a) A. G. Wren, P. A. Gilbert, and M. T. Bowers, *Rev. Sci. Instrum.*, **49**, 531

(1978); (b) M. T. Bowers, P. V. Neilson, P. R. Kemper, and A. G. Wren, *Int. J. Mass Spectrom. Ion Phys.*, **25**, 103 (1977).
(22) D. E. Pearson and J. D. Bruton, *J. Org. Chem.*, **19**, 957 (1954).
(23) M. S. Khardscht and O. Reinmuth, "Grignard Reactions of Nonmetallic Substances", Prentice-Hall, New York, 1954, pp 26, 143.
(24) D. R. Stull and H. Prophet, "JANAF Thermochemical Tables", 2nd ed., NSRDS-NBS 37, U.S. Government Printing Office, Washington, D.C., 1971.
(25) W. F. Bailey and A. S. Monahan, *J. Chem. Educ.*, **55**, 489 (1978).
(26) S. W. Benson, "Thermochemical Kinetics", 2nd ed., Wiley-Interscience, New York, 1976.
(27) (a) L. Batt, K. Christie, R. T. Milne, and A. J. Summers, *Int. J. Chem. Kinet.*, **6**, 877 (1974); (b) S. W. Benson, F. R. Cruickshank, D. M. Golden, G. R. Haugen, H. E. O'Neal, A. S. Rogers, R. Shaw, and R. Walsh, *Chem. Rev.*, **69**, 279 (1969).
(28) A. J. Colussi and S. W. Benson, *Int. J. Chem. Kinet.*, **9**, 295 (1977).
(29) D. H. Fine and J. B. Westmore, *Can. J. Chem.*, **48**, 395 (1970).
(30) T. E. Sharp, J. R. Eyler, and E. Li, *Int. J. Mass Spectrom. Ion Phys.*, **9**, 421 (1972).
(31) T. B. McMahon and J. L. Beauchamp, *J. Phys. Chem.*, **81**, 593 (1977).
(32) J. E. Bartmess, J. A. Scott, and R. T. McIver, Jr., *J. Am. Chem. Soc.*, following paper in this issue.
(33) (a) D. K. Bohme, E. Lee-Ruff, and L. B. Young, *J. Am. Chem. Soc.*, **94**, 5153 (1972); (b) Z. Karpas and F. S. Klein, *Int. J. Mass Spectrom. Ion Phys.*, **18**, 65 (1975).
(34) J. Scott Miller, Ph.D. Dissertation, University of California, Irvine, 1977.
(35) D. J. DeFrees, unpublished results.
(36) S. K. Pollack and W. J. Hehre, *J. Am. Chem. Soc.*, **99**, 4845 (1977).
(37) J. L. Franklin, *Science*, **193**, 725 (1976).
(38) S. W. Benson, F. R. Cruickshank, D. M. Golden, G. R. Haugen, H. E. O'Neal, A. S. Rodgers, R. Shaw, and R. Walsh, *Chem. Rev.*, **69**, 279 (1969).
(39) J. G. Dillard, *Chem. Rev.*, **73**, 589 (1973).

Substituent and Solvation Effects on Gas-Phase Acidities[1]

John E. Bartmess,[2a] Judith A. Scott,[2b] and Robert T. McIver, Jr.*

Contribution from the Department of Chemistry, University of California, Irvine, Irvine, California 92717. *Received February 13, 1979*

Abstract: The structure of a wide variety of Brønsted acids is related to their intrinsic gas-phase acidity. Polarizability is a major factor in the gas phase in the effect of all substituents on anionic centers, often reversing the "polar" effect assigned from solution phase reactivities of both electron-donating and electron-withdrawing groups. Methyl groups interact with anionic centers by a mixture of polar, polarizability, and hyperconjugative interactions. Solvation by dipolar aprotic solvents results in little compression of relative acidities, but water as solvent compresses many substituent effects to one-quarter of their intrinsic value.

Elucidation of the relationship between structure and reactivity has long been a chief goal of physical organic chemistry. The role of solvation in this endeavor has been an uncertain one, since modern structural concepts, though they provide a good framework for analysis of intramolecular interactions between substituent and reactive site, do not give very precise microscopic descriptions of the structure of the medium about the reactants. This is part of the reason that many structure–reactivity correlations deal only with intrinsic structure of the reagents, for which a good mental picture is available, and regard such poorly known factors as the substituent's influence on solvation of the reactive site, or variation of a substituent's intrinsic effect with changing nature of the solvation, as a second-order perturbation. This is certainly justifiable in a great many cases, as the success of linear free-energy relationships attests.[3] It is still surprising, however, when this assumption about the relative importance of intrinsic structure vs. solvation breaks down, as in the results of Brauman and Blair in 1968[4] where solvation was found to reverse the order of intrinsic acidity of the simple aliphatic alcohols.

Brønsted acidities are an excellent choice as a reaction type for investigation of intrinsic structure–reactivity relationships in the absence of solvation. Any molecule containing a hydrogen atom is potentially a Brønsted acid, so a given reaction can be observed with a tremendous variety of substituents. Proton transfer is one of the most conceptually simple reactions known. In the gas phase, there is no solvent leveling[5] to place bounds on the range of reactivities observable. There is also no compression[6] of substituent effects due to the solvent providing part of the stabilization for high-energy species, thus reducing the fraction and absolute magnitude of the intrinsic substituent effect. This allows for observation of substituent effects often too small to measure in solution. In this paper, the body of gas-phase acidity data,[1] measured by pulsed ion cyclotron resonance spectrometry, is analyzed in terms of intrinsic substituent effects. Solvation effects are inferred by differences with known solution acidities.

Results and Discussion

The gas-phase acidities analyzed in this paper are taken from Tables I and III of ref 1 unless otherwise stated. The relative values are believed to be accurate to ±0.2 kcal/mol, and the absolute values to ±2.0 kcal/mol.

Alkyl Effects. In all cases in Table I, increasing the size of the alkyl group is acid strengthening, due to polarizability interactions.[4,7] The effect falls off with distance, although the variety of structures, uncertainty of the exact charge distribution in the delocalized anions, and uncertainty of the mechanism of the interaction[8] prevent testing of the theoretical $1/r^4$ nature of the decrease.[9] The smaller effects in the thiols compared with the alcohols can either be due to this distance effect with the longer C–S bond ($\sim 1/r^{2.4}$ for Me vs. Et), or to a saturation effect[10] where the inherently more stable RS^- anion is less in need of the ion-induced dipole stabilization than the RO^- anion. A saturation effect is also observed for α-methyl substitution into methanol and methanethiol: each successive methyl has a smaller effect. This is not seen for β-methyl substitution into ethanol or 2,2-dimethyl-3-butanol where every new β-methyl increases acidity by a constant amount. Examination of molecular models reveals that a β-methyl in certain configurations can approach more closely to the oxyanion than an α-methyl can, and may as a result be more effective at stabilization due to polarizability, though farther away in bonding terms. The relative acidities of the aliphatic alcohols have been explained in terms of a large polarizability effect and a small, acid-weakening, polar effect.[11] The saturation effect observed for α-methyl, but not β-methyl, substitution may be due to the polar effect being more important in α substitution, or due to the highly variant nature of the polarizability interaction on the intramolecular distance scale.[8] Since polarizability is anisotropic and is important in

0002-7863/79/1501-6056$01.00/0